Peptide neuromodulation of synaptic dynamics in an oscillatory network

Shunbing Zhao

Department of Biological Sciences, Rutgers University, Newark, NJ 07102. shunbing@gmail.com

Amir Farzad Sheibanie

Department of Neuroscience, University of Medicine and Dentistry of New Jersey, Newark, NJ 07102. leo7431@yahoo.com

Myongkeun Oh

Department of Mathematical Sciences, New Jersey Institute of Technology, Newark, NJ 07102. mo42@njit.edu

Pascale Rabbah

Department of Biological Sciences, Rutgers University, Newark, NJ 07102. prabbah@hotmail.com

Farzan Nadim

Department of Mathematical Sciences, New Jersey Institute of Technology and Department of Biological Sciences, Rutgers University, Newark, NJ 07102. farzan@njit.edu

Abbreviated title: Neuromodulation of synaptic dynamics

Corresponding Author:

Farzan Nadim, Rutgers University, Department of Biological Sciences, 195 University Ave., Newark, NJ 07102, Phone (973) 353-1541, Email: farzan@njit.edu

Number of Figures: 8

Number of Words: Abstract 241; Introduction 506; Discussion 1587

Acknowledgments Supported by National Institute of Health Grant MH-60605. AFS was supported by NINDS 1T32NS051157.

Abstract

Neuromodulation of synaptic strength and short-term dynamics can have important consequences for the output of an oscillatory network. Although such effects are documented, few studies have examined neuromodulation of synaptic output in the context of network activity. The crab pyloric bursting oscillations are generated by a pacemaker group that includes the pyloric dilator (PD) neurons. The sole chemical synaptic feedback to this pacemaker group is the inhibitory synapse from the lateral pyloric (LP) neuron, which is comprised of an action-potential-mediated and a graded component. We show that the neuropeptide proctolin unmasks a surprising heterogeneity in its dynamics of the graded component depending on the magnitude of the presynaptic input: it switches the direction of short-term dynamics of this component by changing depression to facilitation. Whether the graded component shows depression or facilitation, however, depends on the amplitude of the slow voltage waveform of the presynaptic LP neuron and is correlated with a putative presynaptic calcium current. The spike-mediated component is strengthened as the baseline membrane potential is increased in control conditions and is also enhanced by proctolin at all baseline potentials. In addition to direct modulation of the synaptic components, proctolin also affects the amplitude of the LP waveform and its action potential frequency, both of which influence synaptic release. Acting through these multiple pathways, proctolin greatly enhances the strength of this synapse under natural biological conditions as evidenced in the significant increase in the synaptic current measured during ongoing oscillations.

Introduction

Short-term synaptic dynamics such as facilitation and depression have been shown to play an important role in shaping the output of neuronal networks (Abbott et al., 1997; Tsodyks et al., 2000; Manor and Nadim, 2001; Zucker and Regehr, 2002; Deeg, 2009). Synaptic plasticity also ensues from modification of synaptic strength by neuromodulators (Ayali et al., 1998; Sakurai and Katz, 2003; Thirumalai et al., 2006). Neuromodulation of the short-term dynamics, reported in many systems (Bristol et al., 2001; Baimoukhametova et al., 2004; Cartling, 2004; Sakurai and Katz, 2009), is considered a form of metaplasticity and can have complex network consequences (Fischer et al., 1997b); yet, little is known about neuromodulation of synaptic dynamics in the context of network oscillations. Synapses often involve distinct components that act at different time scales or involve spike-mediated, graded or asynchronous release (Warzecha et al., 2003; Otsu et al., 2004; Ivanov and Calabrese, 2006). We explore how neuromodulation modifies distinct components of a synapse in an oscillatory network and examine how these modulatory actions shape the combined synapse in the context of network activity.

The crustacean pyloric oscillations are generated in the stomatogastric nervous system (STNS) by a pacemaker group consisting of the gap-junction-coupled anterior burster (AB) and pyloric dilator (PD) neurons that burst in synchrony and inhibit all other pyloric neurons. The sole chemical feedback from the pyloric follower neurons to the pacemakers is the synapse from the lateral pyloric (LP) neuron to the PD neurons, according a key role for this synapse in the regulation of pyloric oscillations (Manor et al., 1997; Mamiya et al., 2003; Weaver and Hooper, 2003). A variety of neuromodulators in the STNS modify the intrinsic properties of individual pyloric neurons (Harris-Warrick et al., 1998; Swensen and Marder, 2000) and the strength and dynamics of synapses among these neurons (Johnson et al., 2005; Johnson et al., 2011). In this study, we demonstrate the ability of the modulatory neuropeptide proctolin to alter the strength and unmask novel dynamics in the LP to PD synapse. Proctolin is released by several projection neurons in the STNS (Nusbaum et al., 2001) and activates a voltage-gated ionic current in several pyloric neurons (Swensen and Marder, 2001). However, the effect of proctolin on the pyloric synapses has not been previously examined. The LP to PD synapse has both

spike-mediated and graded components, as found in other systems (Angstadt and Calabrese, 1991; Pan et al., 2001; Warzecha et al., 2003; Ivanov and Calabrese, 2006). We first characterize the effect of proctolin on the strength and short-term dynamics of the two components of the LP to PD synapse separately. The graded component of this synapse, which depresses in control conditions (Manor et al., 1997), is enhanced and can show facilitation in proctolin, while the spike-mediated component is also strengthened by proctolin. To measure the combined effect of proctolin, we record voltage waveforms of the LP neuron during ongoing activity and use these realistic waveforms in the voltage-clamped LP neuron to unmask the contribution of these changes to total synaptic output in biologically realistic conditions.

Materials and Methods

Preparation and identification of the neurons

Experiments were conducted on the stomatogastric nervous system (STNS) of the crab *Cancer borealis*. Animals were obtained from local markets and maintained in filtered, re-circulating seawater tanks at 10-12 °C. The STNS was dissected out using standard procedures (Blitz et al., 2004; Tohidi and Nadim, 2009). Briefly, the complete isolated STNS (including the stomatogastric ganglion, STG; the esophageal ganglion, OG; and the paired commissural ganglia, CoG; Fig. 1A) was pinned down on a Sylgard-coated Petri dish. The STG was desheathed to facilitate penetration of the pyloric neuron cell bodies. All preparations were continuously superfused with chilled (10-13°C) physiological *Cancer* saline containing (in mM) KCl 11, NaCl 440, $CaCl_2$ 13, $MgCl_2$ 26, Trizma base 11.2, Maleic Acid 5.1, pH=7.4-7.5. Proctolin (Sigma-Aldrich) was dissolved as stock solution in distilled water to a final concentration of 10^{-3} M, divided into aliquots and frozen at –20 °C. The final concentration was made by dissolving the stock solution in *Cancer* saline immediately before use. The dose response effect on the synaptic input-output curve was done by bath applying proctolin from low to high concentration (10^{-9} - 10^{-5} M) in 20 minute intervals. All other applications of proctolin were done at 10^{-6} M. Application of proctolin and other solutions were bath applied by means of a switching port in a continuously flowing superfusion system.

Extracellular recordings from identified motor nerves were made using stainless steel wire electrodes, inserted inside and outside of a petroleum jelly well built to electrically isolate a small section of the nerve, and amplified with a Differential AC amplifier (A-M systems 1700). Intracellular recordings were made from the neuronal cell bodies with sharp glass microelectrodes containing 0.6 M K_2SO_4 and 20 mM KCl (final electrode resistance 20-30 MΩ). Microelectrodes were pulled using a Flaming-Brown P-97 micropipette puller (Sutter Instruments). All intracellular recordings were performed in single-electrode current clamp or two-electrode voltage clamp mode (Axoclamp 2B amplifiers; Molecular Devices). Pyloric neurons were identified according to their stereotypical axonal projections in identified nerves and interactions with other STG neurons (Weimann et al., 1991; Blitz et al., 2008).

Neuromodulatory inputs to the STG

More than 20 different neuromodulators (including several neuropeptides) have been identified in the STNS (Marder and Bucher, 2007). These neuromodulators are released from neurons whose cell bodies reside in anterior ganglia (OG, CoG) and nerves, and project to the STG via the stomatogastric nerve (*stn*) (Nusbaum and Beenhakker, 2002). Several of the neuromodulatory peptides were shown to elicit distinct versions of the pyloric rhythm (Marder and Thirumalai, 2002) and their actions at the network level have been found to be dose- and frequency-dependent (Nusbaum, 2002). In this study, we focused on the neuromodulatory effects of a single, well characterized neuropeptide, proctolin (Hooper and Marder, 1984; Marder et al., 1986; Hooper and Marder, 1987; Golowasch and Marder, 1992; Blitz et al., 1999; Swensen and Marder, 2001).

Effect of proctolin on the strength and dynamics of the LP to PD synapse

Measurements of synaptic output were done by measuring amplitude when there was little variability in the synaptic potential or current amplitudes. In cases where

biological or other conditions resulted in variability of synpatic amplitude (such as during ongoing activity) we measured the total area of the IPSP or IPSC.

In order to study the graded component of the LP to PD synapse, the preparation was superfused with 10^{-7} M tetrodotoxin (TTX; Biotium) to block action potentials and therefore spike-mediated transmission. The LP neuron was two-electrode voltage clamped with a holding potential of -60 mV and stimulated with multiple square pulses of different amplitudes as well as realistic waveforms of different amplitudes and frequencies. Application of realistic waveforms for synaptic measurements were done according to methods we have been previously described (Mamiya et al., 2003; Tseng and Nadim, 2010). Square pulses of fixed 500 ms duration were used to activate the graded component of LP to PD synapse in 10^{-7} M TTX. Graded synaptic responses were used to measure synaptic input-output relationships which were fit with Boltzmann type equations $1/(1+\exp((V_{LP}-V_{half})/k_{half}))$.

To measure spike-mediated transmission, the LP neuron was voltage clamped at a holding potential between -70 and -50 mV and one of the following two methods was used:

1. Short square voltage pulses of fixed 10-ms duration were used to elicit individual spikes and activate the spike-mediated component of the synapse without eliciting graded release. This was made possible because the voltage clamp holding potential prevented graded release which depends on changes in the baseline membrane potential (we confirmed that 10-ms pulses were too short to elicit graded release by showing that no synaptic current was present in the presence of TTX) and, action potentials could be generated by the brief 10-ms pulses without any significant effect on the baseline membrane potential.

2. Antidromic spikes were elicited by stimulating the nerve *lpn* using a pulse stimulator (A-M system isolated pulse stimulator 2100, USA) using 0.5 msec, 3 to 10 V stimuli. The antidromic spikes (which cannot be clamped with somatic electrodes) invade the arborization of the LP neuron and result in synaptic release.

Measurement of putative Ca^{2+} currents were done in the presence of 10^{-7} M TTX and 10 mM TEA and the presynaptic electrodes were loaded with 2M TEA and 2M CsCl to block potassium currents. In order to measure presynaptic Ca^{2+} currents, the experimental protocol was repeated in both normal saline and Mn^{2+} saline (where Ca^{2+} in the physiological saline is substituted with 12.9 mM Mn^{2+} and 0.1 mM Ca^{2+}) and the difference between the presynaptic currents measured in normal saline and in Mn^{2+} saline was reported as a putative Ca^{2+} current. Calcium channel blockers Ni^{2+} and Cd^{2+} were bath applied at concentrations of 1 and 0.2 mM, respectively.

The two PD neurons are anatomically identical and functionally similar; they exhibit similar intrinsic properties and make and receive similar synaptic connections (Miller and Selverston, 1982; Eisen and Marder, 1984; Hooper, 1997; Rabbah et al., 2005; Rabbah and Nadim, 2005; Soto-Treviño et al., 2005). For clarity, the figures in this manuscript only show results from one PD neuron.

Recording, Analysis and Statistics

Data were acquired using pClamp 9 software (Molecular Devices) or the Scope software (available at http://stg.rutgers.edu/software developed in the Nadim laboratory), sampled at 4 kHz and saved on a PC using a PCI-6070-E data acquisition board (National Instruments). Statistical and graphical analyses were done using Sigmastat 3.0 (Aspire Software) and Origin 7.0 (OriginLab). Reported statistical significance indicated that the achieved significance level p was below the critical significance level α=0.05. All error bars shown and error values reported denote standard deviations.

Results

During the ongoing pyloric rhythm, the LP and PD neurons fire in alternation (Fig. 1B; left panel). Removal of descending modulatory inputs to the STG (decentralization) disrupts the pyloric rhythm as the alternating oscillation of the LP and PD neuron becomes slow and irregular (Fig. 1B; middle panel; see also (Nusbaum and Beenhakker, 2002)). As shown in previous studies (Marder et al., 1986; Nusbaum and Marder, 1989a), bath application of proctolin enhances the pyloric rhythm by increasing the amplitude of the slow wave oscillation of the LP and PD neurons and increasing the spike frequency and number of spikes per burst (Fig. 1B; right panel). It is known that proctolin enhances the bursting activity of the LP and pacemaker neurons by eliciting a voltage-gated inward current (Golowasch and Marder, 1992; Swensen and Marder, 2000). The LP to PD synapse is the only chemical synaptic feedback to the pyloric pacemaker neurons. As such, this synapse is in a key position to affect the frequency and phase relationships of the pyloric network (Eisen and Marder, 1982; Weaver and Hooper, 2003; Mamiya and Nadim, 2004, 2005). Our goal in this study is to characterize the neuromodulation of the LP to PD synapse by proctolin. An examination of the size of the IPSPs resulting from this synapse (gray regions marked in Fig. 1B) shows that during ongoing oscillations proctolin strengthens the synapse compared to control conditions (Fig. 1D; Student's t-test, $p<0.01$, $N=5$).

The LP to PD synapse consists of two components: a spike-mediated component that manifests as unitary IPSPs in response to individual action potentials in the presynaptic LP neuron (clearly seen in the Decentralized PD neuron trace in Fig. 1B) and a graded (non-spike-mediated) component (Manor et al., 1997; Ayali et al., 1998; Mamiya and Nadim, 2004). We first examined the effects of proctolin on these two components of LP to PD synapse separately.

To measure the graded component of the LP to PD synapse, the preparation was bathed with 10^{-7} M TTX to remove action potentials and therefore block spike-mediated transmission. The LP neuron was voltage clamped to a holding potential of –60 mV and then injected with a series of 500 ms depolarizing square voltage pulses with increasing amplitudes, in control and after bath application of 10^{-6} M proctolin, and the resulting

IPSPs were recorded in the PD neuron (Fig. 2). The IPSP amplitude increased as the amplitude of the LP neuron depolarizations increased in both control and proctolin, as expected from a graded synapse. The amplitudes of the graded IPSPs (gIPSPs) were larger in proctolin, indicating the strengthening of the LP to PD synapse by proctolin. The enhancement of the synaptic strength was reversible after a 45 minute wash although the synapse often appeared slower to activate at high presynaptic voltages after wash (Fig. 2A).

The synaptic input-output curve constructed using the peak amplitudes of the gIPSPs showed a sigmoidal dependency on the presynaptic voltage for both control and proctolin (Figs. 2B and 2C). The amplitudes of gIPSPs were augmented in proctolin in a dose dependent manner but saturated at 10^{-6} M (Fig. 2B) which is the dose typically used in previous studies of proctolin in this system (Nusbaum and Marder, 1989a; Swensen and Marder, 2000). All subsequent data reported in this study is with 10^{-6} M proctolin.

Proctolin significantly strengthened gIPSPs of the LP to PD synapse for presynaptic amplitudes $\geq$ 35 mV (two-way ANOVA post-hoc Tukey analysis, $p < 0.01$ for $V_{LP} = -35$ to -10 mV; N=6). To examine the effect of proctolin on the synaptic input-output curve, the amplitude of the individual gIPSPs in each preparation was normalized to the gIPSP measured in response to the highest presynaptic amplitude (Fig. 2D). Each data point in Fig. 2D indicates a single measurement in six preparations and these measurements were fit with Boltzmann type equations (see Methods). We found that proctolin shifts the midpoint of the input-output curve by about 5.5 mV to more negative membrane potentials (V_{half} in mV—Ctrl: -29.0±0.11; Proc: -35.4±0.14; Wash: -28.0 ±0.44; One-way ANOVA, $p<0.001$) but did not significantly change the slope of this curve, although the slope became shallower after wash (k_{half} in mV—Ctrl: -3.11±0.10; Proc: -2.83±0.12; Wash: -6.36 ±0.45, p=0.2 for Ctrl vs. Wash).

The LP to PD synapse has been previously shown to display short-term depression (Manor et al., 1997). To examine whether proctolin modifies the dynamics of this synapse, we injected a train of voltage pulses with different amplitudes from a holding potential of -60 mV into the LP neuron and recorded the gIPSPs in the PD neuron in control saline and in the presence of 10^{-6} M proctolin. In almost all recordings,

the amplitude of the gIPSP did not change subsequent to the 4th pulse and therefore we refer to the gIPSP in response to the 5th pulse as the steady-state gIPSP. An example of the synaptic response to trains of pulses with two different amplitudes in control and proctolin is shown in Fig. 3A. As seen in this figure, in response to 40 mV pulses, the steady-state gIPSP was always slightly smaller than the 1st pulse gIPSP, indicating synaptic depression, in both control (gray) and proctolin (pink). In contrast, the gIPSPs elicited with 20 mV presynaptic pulses were qualitatively different: in this case, the gIPSPs in the PD neuron either did not change or showed slight depression in control, but facilitation in proctolin: the response to the 1st pulse was relatively small but became much larger by the 3rd pulse. Figure 3B shows the ratio of the 5th to the 1st mean gIPSP amplitude (A_5/A_1) calculated for all presynaptic depolarizations with an inter-pulse interval of 500 ms. In control conditions, the ratio A_5/A_1 was slightly less than one for all values of presynaptic pulse amplitudes (ΔV_{LP}), indicating that the synapse was always depressing. In contrast, in the presence of proctolin, the A_5/A_1 ratios in response to pulse amplitudes between 20 and 24 mV were greater than 1 while the ratios in response to larger pulse amplitudes were less than 1, indicating facilitation and depression, respectively (2-way ANOVA with post hoc Tukey test showing $p<0.001$ between ctrl and proctolin and $p<0.008$ between control and wash for $\Delta V_{LP} = 20$, 22 and 24 mV; not significant at other ΔV_{LP}). For ΔV_{LP} values below 20 mV the gIPSP was typically too small (< 1 mV; see Fig. 2C) to reliably measure short-term dynamics which explains the large error bars seen at these voltages. These experiments showed that proctolin acts at the level of the synapse, causing this depressing synapse to become facilitating in response to low-amplitude presynaptic depolarizations, while maintaining a low level of depression with high-amplitude depolarizations.

We hypothesized that the appearance of synaptic facilitation with low-amplitude presynaptic voltage pulses in the presence of proctolin was due to additional presynaptic calcium currents. To examine this hypothesis, we applied 20 mV pulses in the LP neuron to correlate the synaptic response with presynaptic Ca^{2+} currents in the LP neuron. Each experimental protocol was first performed in normal saline and after blocking Ca^{2+} currents (and therefore synaptic transmission), in both control and proctolin, by substituting the Ca^{2+} with Mn^{2+} (see Methods). In all conditions, we made simultaneous

measurements of the presynaptic current (Fig. 4A, I_{LP}) and the postsynaptic potential (Fig. 4A, V_{PD}). The difference between the presynaptic currents measured in normal saline (labeled Ca^{2+}) and in Mn^{2+} saline was measured as a putative calcium current (Fig. 4A, ΔI_{LP}).

In normal saline, there was little synaptic response in control conditions and no apparent synaptic plasticity was observed (Fig. 4A, left panel and Fig 3A Ctl black trace). In contrast, the synaptic response was strengthened and showed facilitation in proctolin (Fig. 4A, right panel and Fig 3A Proc dark red trace). For clarity, V_{PD} is not shown in Mn^{2+} saline because there was no synaptic transmission in either control or proctolin. The putative calcium current was small in control conditions and its amplitude showed no obvious variation among the different voltage pulses (Fig. 4A, left panel, ΔI_{LP}). In contrast, in the presence of proctolin, this current increased with each subsequent pulse, indicating accumulation of Ca^{2+} currents (Fig. 4A, right panel, ΔI_{LP}). We used these data to examine whether the putative Ca^{2+} current ΔI_{LP} measured in proctolin may underlie the increase in the amplitude of the gIPSPs thus resulting in the observed facilitation. The peak of the gIPSPs in response to low-amplitude presynaptic pulses were often highly variable or hard to discern, especially in control where the gIPSPs were small (Fig 4A, V_{PD} trace). Due to the variability in the peak current and the peak gIPSPs and the fact that the measured presynaptic currents were at times contaminated with outward currents, we compared the mean values of ΔI_{LP} and gIPSP during each pulse. There was a modest positive correlation between the presynaptic inward current and the postsynaptic potentials (Fig. 4B, linear fit: $R=0.69$, $P<0.001$, $N=9$), supporting the hypothesis that the facilitation in proctolin is due to a proctolin-induced accumulation of additional calcium current in the LP neuron.

We also examined whether proctolin affects the strength of the spiked-mediated component of the LP to PD synapse. In order to elicit single spike-mediated IPSPs (sIPSP), the presynaptic LP neuron was voltage clamped at a holding potential of -60 mV and stimulated with a very short voltage pulse of duration 10 ms and amplitude 30 mV to elicit a single action potential (Fig. 5A). The short voltage pulses ensured that there was no graded release (which we also verified by repeating the same protocol in TTX and observing no IPSP; see Materials and Methods). Bath application of proctolin

significantly enhanced the amplitude of the unitary sIPSP values (Figs. 5A and 5B; Student's t-test, $p<0.001$; N=6).

Although a 10 ms voltage pulse applied even at 40 mV amplitude in the presynaptic LP neuron never produced any graded synaptic release (IPSP amplitude 0 mV in TTX; N=3), we observed that the amplitude of sIPSPs in response to single action potentials elicited by the 10 ms voltage pulse in normal saline increased if the amplitude of this short presynaptic voltage pulse was increased (to peak voltages V_{LP} = -40, -30, -20, -10 mV; Figs. 5C and 5D, Control). Additionally, bath application of proctolin significantly increased the sIPSP amplitude for all values of the presynaptic pulse amplitudes (Fig. 5C and 5D; two-way ANOVA post-hoc Tukey analysis, $p<0.05$, N=8).

To completely exclude the possibility that these results were contaminated by the graded component of the LP to PD synapse, we also measured sIPSPs elicited by antidromic spikes while voltage clamping the LP neuron soma at a constant holding potentials in the presence and absence of proctolin. To elicit antidromic spikes, we stimulated the lateral pyloric nerve (*lpn*) which contains the axon of the LP neuron but not that of the PD neuron (Fig. 5E). The stimulus-induced antidromic spikes propagated back to the STG where they resulted in synaptic release (Fig. 5F). It is known that the baseline potential of the presynaptic neuron can have a significant effect on the amplitude of the spike-mediated PSPs (Nicholls and Wallace, 1978; Ivanov and Calabrese, 2003). We voltage clamped the LP neuron at different holding potentials below spike threshold (V_{LP}=-70, -60, -55, and -50 mV) and recorded the sIPSPs in the PD neuron in control and in the presence of bath-applied proctolin. We found that, as the holding potential of the LP neuron was increased, the amplitude of sIPSPs in the PD neuron also increased in both control and 10^{-6} M proctolin. Additionally, as in the protocol of Fig. 5B, the sIPSPs were larger in the presence of proctolin in comparison to control (Fig. 5G; two-way RM-ANOVA, $p<0.05$, N=5).

It has been suggested that calcium accumulation through low-threshold calcium channels activated by subthreshold membrane potential depolarization may result in enough background calcium in the presynaptic neuron to enhance spike-mediated release (Ivanov and Calabrese, 2003). Bath application of Ni^{2+} is known to block a number of

low-threshold calcium channels (Lee et al., 1999; Perez-Reyes, 2003), including those responsible for graded transmission in leech heart interneurons (Ivanov and Calabrese, 2006). We examined the effects of Ni^{2+} on the amplitudes of sIPSPs in the LP to PD synapse. We found that sIPSPs (elicited by 10 ms voltage pulses with different amplitudes similar to Fig. 5B) were weakened by bath application of Ni^{2+} by 40-75% (two-way ANOVA, $p<0.05$, N=5) but continued to be enhanced with baseline amplitude (not shown; Ctrl: from 0.8±0.6 at 10 mV amp to 8.5±1.5 mV at 40 mV amp; Ni^{2+}: from 0.9±0.4 at 10 mV amp to 4.8±0.4 mV at 40 mV amp; N=5). It was often difficult to assess the effect of Ni^{2+} on synaptic transmission because long bath application it usually resulted in membrane potential oscillations and activation of the pyloric rhythm even in the presence of TTX (Zirpel et al., 1993). Yet, these results suggest that although an increase in the background calcium in the presynaptic neuron might cause the increase of the sIPSP amplitude as the baseline membrane potential increases, such background calcium is only partially due to Ni^{2+}-sensitive low-threshold calcium channels.

We also examined the effect of proctolin on the short-term dynamics of the sIPSPs. The LP neuron was clamped at a holding potential of -50 mV and the *lpn* was stimulated to produce two successive antidromic spikes and the inter-spike intervals was varied (ISI: 30, 50, 100, 250, 500 ms). Because the stimulus artifact often interfered with the measurement of the sIPSPs with short ISIs, in this protocol we also voltage clamped the postsynaptic PD neuron with two electrodes at a holding potential of -50 mV and measured the spike-mediated synaptic currents (sIPSCs). The sIPSCs were measured and averaged for 10 repeated trials at each ISI value in each experiment and the resulting average amplitude was used as a single data point. As expected, the sIPSC amplitude was significantly strengthened by proctolin (Ctrl: 0.49±0.02 nA, Proc: 1.3±0.1 nA; Student's t-Test, $P<0.01$, N=4; Fig. 6A). To measure the extent of synaptic dynamics, we measured the ratio of the peaks of second to first sIPSC. The sIPSCs of LP to PD synapse exhibited short-term depression in both control and proctolin at shorter ISIs (Fig. 6B). However, there was no difference in depression between control and proctolin (exponential fit curves $y = 1 - Ae^{-x/B}$: Control A=0.23, B=125; Proctolin A=0.15, B=167).

So far, our results demonstrated that proctolin can enhance both graded and spike-mediated components of the LP to PD synapse. A natural question is how the total IPSC is affected by proctolin. To explore this question we decentralized the preparation (Fig. 1B), voltage clamped the LP neuron at a holding potential of -60 mV and applied a voltage profile constructed using a pre-recorded realistic LP neuron waveform as we have done in previous studies (Manor et al., 1997; Mamiya and Nadim, 2004; Johnson et al., 2005; Rabbah and Nadim, 2007). The LP waveform was applied to the voltage clamped LP soma periodically with a cycle period of 1 s and with a total amplitude of 26 mV (as measured in the recording of the waveform) or 39 mV (1.5 times the recorded amplitude). The resulting IPSP was measured in the PD neuron in control saline or in the presence of proctolin (Fig. 7). When the measurements were done in normal saline (i.e., without TTX), the simulated action potentials of the realistic waveform resulted in real action potentials in the presynaptic LP neuron which could be seen on the extracellular recordings of the nerve *lvn* (Fig. 7A). As a result, the IPSP measured in these conditions was a combination of both graded and spike-mediated components. Additionally, the number and frequency of action potentials were the same in control and proctolin because each (simulated) action potential of the prerecorded waveform elicited an action potential in the LP neuron.

To examine how much of the total IPSP was due to the graded component in the different conditions we repeated these measurements in TTX. In these conditions, action potentials were blocked and therefore the spike-mediated IPSP was removed (Figs. 7B and 7D). Note that the simulated action potentials of the pre-recorded waveform were still artificially played back in the voltage clamped LP neuron but, in TTX, these do not result in biological action potentials. Application of the realistic waveform in TTX with total amplitude of 26 mV (same as recorded amplitude) resulted in synaptic facilitation of the gIPSP in proctolin (gray V_{PD} trace) but not control saline (gray V_{PD} trace). In contrast, application of the waveform at 39 mV resulted in slight depression of the gIPSP both in control (black) and in proctolin (red). The effect of presynaptic waveform amplitude on synaptic dynamics is similar to that reported with the pulse waveforms shown in Fig. 4. Note that synaptic facilitation was never observed in TTX-free saline but this may be due

to the fact that, in a decentralized preparation, the LP neuron always has some baseline activity (Fig. 1B) and the synapse cannot be measured in naïve conditions.

We compared the IPSP amplitudes after at least five cycles of the realistic waveform application (circled region in Figs. 7A and 7B) to avoid measuring the transients. Increasing the amplitude of the presynaptic waveform resulted in a larger total IPSP in the PD neuron and proctolin always increased the synaptic amplitude in each preparation (Fig. 7C). On average, both waveform amplitude and the presence of proctolin significantly increased the total synaptic IPSP amplitude (Fig. 7E; two-way RM-ANOVA; $p<0.05$). In TTX, the realistic waveform at 26 mV amplitude did not produce a significant gIPSP in control saline but did so when the amplitude was increased. Additionally, proctolin increased the amplitude of the gIPSP measured with the realistic waveform (not shown; two-way RM-ANOVA; $p<0.05$).

Although our characterization of the components of the LP to PD synapse under controlled conditions where we prescribe the presynaptic waveform provides insight into the actions of the modulator proctolin on this synapse, the effect of proctolin on this synapse should also be characterized under more natural biological conditions. As a first step in exploring these more biologically realistic effects, we measured the LP to PD synaptic currents during ongoing pyloric oscillations. To measure the biological IPSCs, one of the two PD neurons was voltage clamped at -50 mV during ongoing pyloric activity and the IPSCs were measured in control and proctolin (Fig. 8A). In the pyloric network, PD neurons and the pacemaker AB neuron are electrically coupled. Although one PD was voltage clamped, it was still coupled to the other PD and to the AB neuron. We ensured that the pyloric cycle period was matched between control and proctolin conditions (compare the extracellular recordings from *lvn*) by injecting, when necessary, a small DC current in the second PD neuron to speed up or slow down the oscillation to a cycle period of 1 s. The synaptic response in the PD neuron was measured by integrating I_{PD} from the end of the PD burst to the start of the consequent PD burst (vertical dashed line in Fig. 8A). As expected, the total biological IPSC strength was significantly larger in proctolin than control or wash (one-way ANOVA, $p<0.01$, N=5, Fig. 8B).

Discussion

In central pattern generator networks, activity-dependent modification of synaptic strength can be crucial in determining the activity phase of the network neurons and, consequently the activity pattern of the effector muscles. Understanding the actions of neuromodulators on network activity requires knowledge of how synaptic strength is changed in the context of this activity. This requires a characterization of the neuromodulator modification of both synaptic strength and its short-term dynamics.

The LP to PD synapse is the sole chemical feedback synapse to the pyloric pacemaker neurons and, as such, its neuromodulation can have important consequences for network output. We found that both the spike-mediated and graded components of the LP to PD synapse are strengthened by proctolin. Interestingly, proctolin unmasks a surprising heterogeneity in its dynamics of the graded component depending on the magnitude of the presynaptic input. In the presence of proctolin, low-amplitude presynaptic stimuli switch the short-term dynamics of this graded component from depression to facilitation. The shift to facilitation is correlated with an increase in a putative presynaptic calcium current. We also found that the spike-mediated component of the LP to PD synapse is dependent on the baseline presynaptic membrane potential from which action potentials are generated and that, at all membrane potentials, the spike-mediated component is enhanced by proctolin. Finally, by voltage-clamping the presynaptic neuron using pre-recorded realistic waveforms as well as measuring of the synaptic current during ongoing activity, we demonstrated that proctolin enhances the combined synaptic output in the context of network oscillations.

Modulatory actions of proctolin

The crab pyloric network is modulated by over twenty neurotransmitters and hormones (Marder et al., 2005). Among the best studied of these modulators is the neuropeptide proctolin: all proctolinergic modulatory projection neurons in the crab STNS are known and the network actions of many of these neurons have been characterized (Nusbaum and Beenhakker, 2002). Proctolin is known to strongly excite and modify the pyloric rhythm (Marder et al., 1986; Hooper and Marder, 1987; Nusbaum

and Marder, 1989b), an effect that is at least partly due to the activation of a voltage-dependent non-specific cation channel in pyloric neurons (Golowasch and Marder, 1992; Swensen and Marder, 2001). However, the effect of proctolin on the pyloric synapses has not been previously examined.

Proctolin exerts its effects through binding to G-protein coupled receptors and subsequently activating downstream signaling pathways (Johnson et al., 2003). Studies in insect and crayfish muscle have shown that using second messengers IP_3 and cAMP, proctolin can increase intracellular calcium concentrations by modulating voltage-dependent or voltage-independent channels (Baines et al., 1990; Bishop et al., 1991; Wegener and Nassel, 2000). Proctolin, however, does not appear to cause an increase of cAMP levels in STG neurons (Flamm et al., 1987; Hempel et al., 1996), nor did we find an effect of bath application of membrane-pemeable 8-Bromo-cAMP in changing the synaptic strength or dynamics (not shown). The cGMP pathway has been shown to be involved in the potentiation of crustacean muscle contraction by proctolin (Philipp et al., 2006). In the STNS, however, there is still little known about the second messenger pathways underlying the modulatory actions of proctolin.

Neuromodulation of short-term synaptic dynamics

Short-term synaptic dynamics have been shown to play roles in behavioral habituation and sensitization (Stopfer and Carew, 1996; Zucker, 1999), filtering (Lisman, 1997; Zador and Dobrunz, 1997; Dittman et al., 2000; Lindner et al., 2009), neural information processing and in the control of network activity (Bertram, 1997; Buonomano, 2000; Matveev and Wang, 2000; Nadim and Manor, 2000; Hanson and Jaeger, 2002; Lewis and Maler, 2002). Much of the understanding of the neuromodulation of short-term synaptic dynamics has come from invertebrate studies (Fischer et al., 1997a; Bristol et al., 2001; Logsdon et al., 2006; Sakurai et al., 2006; Sakurai and Katz, 2009), yet such effects have also been observed in vertebrate synapses (Gil et al., 1997; Giocomo and Hasselmo, 2007; Parker and Gilbey, 2007). While the effects of modulators on synaptic dynamics are documented, few studies other than the

current one have shown a modulator to switch the direction of synaptic dynamics from depression to facilitation (Barriere et al., 2008).

It is noteworthy that facilitation of the graded LP to PD synapse in the presence of proctolin is different from classical synaptic facilitation which depends on the timing of the presynaptic activity and not its amplitude. Other, non-proctolin-mediated, modulatory and projection-neuron actions are known to affect the amplitude of LP neuron activity (Norris et al., 1996; Johnson et al., 2005). It is possible that retaining synaptic depression with large presynaptic amplitudes and facilitation with low amplitudes in the presence of proctolin may function to buffer the synaptic strength in response to changes in the amplitude of the LP oscillations in response to these other inputs, so that variations in the LP neuron voltage amplitude do not produce large changes in its synaptic output to the pacemaker neurons. As such, an amplitude-dependent switch from depression to facilitation in the LP to PD synapse may help maintain the stability of the rhythmic pyloric motor output.

Potential mechanisms underlying the facilitation caused by proctolin

Short-term facilitation is generally governed by the properties of the presynaptic neuron (Zucker and Regehr, 2002). Our results also support a presynaptic mechanism because the increase in the synaptic strength in response to a train of pulses is correlated with the slow activation of a presynaptic Mn^{2+}-sensitive inward current. This current is likely to be a calcium current activated by proctolin, although a definitive proof requires additional experiments beyond the scope of this study. Using a biophysical model of synaptic release, we have found that proctolin actions on the LP to PD synapse can be explained by the activation of a low-threshold voltage-gated calcium current with slow activation and inactivation kinetics (Zhou et al., 2007). Yet, other mechanisms may underlie the appearance of the putative calcium current. For example, as mentioned above, proctolin activates a non-specific cation channel in pyloric neurons (Golowasch and Marder, 1992; Swensen and Marder, 2000) which is presumed to have a pore block by calcium ions (Golowasch and Marder, 1992; Swensen and Marder, 2000). It has been shown that the ion that produces a pore block—such as Mg^{2+} in NMDA channels—can

also permeate into the cytoplasm (Stout et al., 1996). This allows the possibility that the proctolin-activated channel has some permeability for calcium, whose accumulation leads to the observed synaptic facilitation. These two hypothetical mechanisms could be distinguished by imaging calcium entry in the presynaptic LP neuron in the presence or absence of calcium channel blockers.

The role of baseline membrane potential on spike-mediated transmission

The dependence of spike-mediated synapses on baseline membrane potential has been shown in many systems including mammalian central synapses (Nicholls and Wallace, 1978; Ivanov and Calabrese, 2003; Alle and Geiger, 2006; Ivanov and Calabrese, 2006; Shu et al., 2006). In leech heart interneurons, it is known that low-threshold calcium currents activate the graded component of synaptic release, whereas spike-mediated synaptic transmission is triggered by high-threshold calcium currents (Angstadt and Calabrese, 1991; Lu et al., 1997). In these neurons, an increase in the background calcium levels at the presynaptic site due to the membrane potential depolarization is correlated with the increase in the amplitude of the spike-mediated IPSPs (Ivanov and Calabrese, 2006). We suspect a similar mechanism to be at work for the LP to PD synapse although, unlike the leech synapses where Cd^{2+} can be used to specifically block the high-threshold calcium current and thus only spike-mediated release, Cd^{2+} blocks both components of the LP to PD synapse. An additional enhancement of the background calcium levels by proctolin through voltage-gated calcium channels, intrinsic calcium release or through the modulator-activated channels can potentially explain the strengthening of the spike-mediated component with little effect on its dynamics.

The effect of proctolin on combined transmission using realistic waveforms

Graded transmission is thought to be the major form of synaptic communication among pyloric neurons (Graubard et al., 1983; Hartline et al., 1988; Manor et al., 1997). This is supported by the observation that pyloric oscillations can be produced in the presence of neuromodulators even when action potentials are blocked (Raper, 1979; Anderson and Barker, 1981). Although many pyloric synapses appear to be purely graded,

others, such as the LP to PD synapse, have a clear spike-mediated component. Interestingly, when we played back the LP neuron realistic waveform at the amplitude which it was recorded, we saw little graded transmission in control conditions yet this synaptic component was clearly present in proctolin (Fig. 7C). It is therefore possible that under different modulatory conditions one or the other component of synaptic transmission is dominant in affecting the total synaptic strength.

It is common for neuromodulators to change the activity waveform of bursting neurons (Marder and Thirumalai, 2002). Proctolin, for example, increases the amplitude of the LP neuron burst waveform and its spike frequency (Hooper and Marder, 1984 ; Nusbaum and Marder, 1989b). The LP to PD synapse is significantly enhanced if the amplitude of the LP waveform is increased, independent of any direct actions of proctolin on the synapse (Fig. 7). This enhancement is due both to the increase in strength of the graded component with presynaptic voltage amplitude and because the spike-mediated component is enhanced when the baseline membrane potential is increased. However, as we have shown, proctolin also directly enhances these two synaptic components. Thus, during natural ongoing oscillations, the proctolin enhancement of the LP to PD synapse results from a combination of direct modulation as well as enhanced release due to the increase in the presynaptic waveform amplitude and spike frequency.

References

Abbott LF, Varela JA, Sen K, Nelson SB (1997) Synaptic depression and cortical gain control. Science 275:220-224.

Alle H, Geiger JR (2006) Combined analog and action potential coding in hippocampal mossy fibers. Science 311:1290-1293.

Anderson WW, Barker DL (1981) Synaptic mechanisms that generate network oscillations in the absence of discrete postsynaptic potentials. J Exp Zool 216:187-191.

Angstadt JD, Calabrese RL (1991) Calcium currents and graded synaptic transmission between heart interneurons of the leech. J Neurosci 11:746-759.

Ayali A, Johnson BR, Harris-Warrick RM (1998) Dopamine modulates graded and spike-evoked synaptic inhibition independently at single synapses in pyloric network of lobster. J Neurophysiol 79:2063-2069.

Baimoukhametova DV, Hewitt SA, Sank CA, Bains JS (2004) Dopamine modulates use-dependent plasticity of inhibitory synapses. J Neurosci 24:5162-5171.

Baines RA, Lange AB, Downer RG (1990) Proctolin in the innervation of the locust mandibular closer muscle modulates contractions through the elevation of inositol trisphosphate. J Comp Neurol 297:479-486.

Barriere G, Tartas M, Cazalets JR, Bertrand SS (2008) Interplay between neuromodulator-induced switching of short-term plasticity at sensorimotor synapses in the neonatal rat spinal cord. J Physiol 586:1903-1920.

Bertram R (1997) A simple model of transmitter release and facilitation. Neural Comput 9:515-523.

Bishop CA, Krouse ME, Wine JJ (1991) Peptide cotransmitter potentiates calcium channel activity in crayfish skeletal muscle. J Neurosci 11:269-276.

Blitz DM, Beenhakker MP, Nusbaum MP (2004) Different sensory systems share projection neurons but elicit distinct motor patterns. J Neurosci 24:11381-11390.

Blitz DM, Christie AE, Coleman MJ, Norris BJ, Marder E, Nusbaum MP (1999) Different proctolin neurons elicit distinct motor patterns from a multifunctional neuronal network. J Neurosci 19:5449-5463.

Blitz DM, White RS, Saideman SR, Cook A, Christie AE, Nadim F, Nusbaum MP (2008) A newly identified extrinsic input triggers a distinct gastric mill rhythm via activation of modulatory projection neurons. J Exp Biol 211:1000-1011.

Bristol AS, Fischer TM, Carew TJ (2001) Combined effects of intrinsic facilitation and modulatory inhibition of identified interneurons in the siphon withdrawal circuitry of Aplysia. J Neurosci 21:8990-9000.

Buonomano DV (2000) Decoding temporal information: A model based on short-term synaptic plasticity. J Neurosci 20:1129-1141.

Cartling B (2004) Neuromodulatory control of neocortical microcircuits with activity-dependent short-term synaptic depression. Journal of Biological Physics 30:261-284.

Deeg KE (2009) Synapse-specific homeostatic mechanisms in the hippocampus. J Neurophysiol 101:503-506.

Dittman JS, Kreitzer AC, Regehr WG (2000) Interplay between facilitation, depression, and residual calcium at three presynaptic terminals. J Neurosci 20:1374-1385.

Eisen JS, Marder E (1982) Mechanisms underlying pattern generation in lobster stomatogastric ganglion as determined by selective inactivation of identified neurons. III. Synaptic connections of electrically coupled pyloric neurons. J Neurophysiol 48:1392-1415.
Eisen JS, Marder E (1984) A mechanism for production of phase shifts in a pattern generator. J Neurophysiol 51:1375-1393.
Fischer TM, Zucker RS, Carew TJ (1997a) Activity-dependent potentiation of synaptic transmission from L30 inhibitory interneurons of aplysia depends on residual presynaptic Ca2+ but not on postsynaptic Ca2+. J Neurophysiol 78:2061-2071.
Fischer TM, Blazis DE, Priver NA, Carew TJ (1997b) Metaplasticity at identified inhibitory synapses in Aplysia. Nature 389:860-865.
Flamm RE, Fickbohm D, Harris-Warrick RM (1987) cAMP elevation modulates physiological activity of pyloric neurons in the lobster stomatogastric ganglion. J Neurophysiol 58:1370-1386.
Gil Z, Connors BW, Amitai Y (1997) Differential regulation of neocortical synapses by neuromodulators and activity. Neuron 19:679-686.
Giocomo LM, Hasselmo ME (2007) Neuromodulation by glutamate and acetylcholine can change circuit dynamics by regulating the relative influence of afferent input and excitatory feedback. Mol Neurobiol 36:184-200.
Golowasch J, Marder E (1992) Proctolin activates an inward current whose voltage dependence is modified by extracellular Ca2+. J Neurosci 12:810-817.
Graubard K, Raper JA, Hartline DK (1983) Graded synaptic transmission between identified spiking neurons. J Neurophysiol 50:508-521.
Hanson JE, Jaeger D (2002) Short-term plasticity shapes the response to simulated normal and parkinsonian input patterns in the globus pallidus. J Neurosci 22:5164-5172.
Harris-Warrick RM, Johnson BR, Peck JH, Kloppenburg P, Ayali A, Skarbinski J (1998) Distributed effects of dopamine modulation in the crustacean pyloric network. Ann N Y Acad Sci 860:155-167.
Hartline DK, Russell DF, Raper JA, Graubard K (1988) Special cellular and synaptic mechanisms in motor pattern generation. Comp Biochem Physiol C 91:115-131.
Hempel CM, Vincent P, Adams SR, Tsien RY, Selverston AI (1996) Spatio-temporal dynamics of cyclic AMP signals in an intact neural circuitm. Nature 384:166-169.
Hooper SL (1997) Phase maintenance in the pyloric pattern of the lobster (Panulirus interruptus) stomatogastric ganglion. J Comput Neurosci 4:191-205.
Hooper SL, Marder E (1984) Modulation of a central pattern generator by two neuropeptides, proctolin and FMRFamide. Brain Res 305:186-191.
Hooper SL, Marder E (1987) Modulation of the lobster pyloric rhythm by the peptide proctolin. J Neurosci 7:2097-2112.
Ivanov AI, Calabrese RL (2003) Modulation of spike-mediated synaptic transmission by presynaptic background Ca2+ in leech heart interneurons. J Neurosci 23:1206-1218.
Ivanov AI, Calabrese RL (2006) Spike-mediated and graded inhibitory synaptic transmission between leech interneurons: evidence for shared release sites. J Neurophysiol 96:235-251.

Johnson BR, Schneider LR, Nadim F, Harris-Warrick RM (2005) Dopamine modulation of phasing of activity in a rhythmic motor network: contribution of synaptic and intrinsic modulatory actions. J Neurophysiol 94:3101-3111.
Johnson BR, Brown JM, Kvarta MD, Lu JY, Schneider LR, Nadim F, Harris-Warrick RM (2011) Differential modulation of synaptic strength and timing regulate synaptic efficacy in a motor network. J Neurophysiol 105:293-304.
Johnson EC, Bohn LM, Barak LS, Birse RT, Nassel DR, Caron MG, Taghert PH (2003) Identification of Drosophila neuropeptide receptors by G protein-coupled receptors-beta-arrestin2 interactions. J Biol Chem 278:52172-52178.
Lee JH, Gomora JC, Cribbs LL, Perez-Reyes E (1999) Nickel block of three cloned T-type calcium channels: low concentrations selectively block alpha1H. Biophys J 77:3034-3042.
Lewis JE, Maler L (2002) Dynamics of electrosensory feedback: short-term plasticity and inhibition in a parallel fiber pathway. J Neurophysiol 88:1695-1706.
Lindner B, Gangloff D, Longtin A, Lewis JE (2009) Broadband coding with dynamic synapses. J Neurosci 29:2076-2088.
Lisman JE (1997) Bursts as a unit of neural information: making unreliable synapses reliable. Trends Neurosci 20:38-43.
Logsdon S, Johnstone AF, Viele K, Cooper RL (2006) Regulation of synaptic vesicles pools within motor nerve terminals during short-term facilitation and neuromodulation. J Appl Physiol 100:662-671.
Lu J, Dalton JFt, Stokes DR, Calabrese RL (1997) Functional role of Ca2+ currents in graded and spike-mediated synaptic transmission between leech heart interneurons. J Neurophysiol 77:1779-1794.
Mamiya A, Nadim F (2004) Dynamic interaction of oscillatory neurons coupled with reciprocally inhibitory synapses acts to stabilize the rhythm period. J Neurosci 24:5140-5150.
Mamiya A, Nadim F (2005) Target-specific short-term dynamics are important for the function of synapses in an oscillatory neural network. J Neurophysiol 94:2590-2602.
Mamiya A, Manor Y, Nadim F (2003) Short-term dynamics of a mixed chemical and electrical synapse in a rhythmic network. J Neurosci 23:9557-9564.
Manor Y, Nadim F (2001) Synaptic depression mediates bistability in neuronal networks with recurrent inhibitory connectivity. J Neurosci 21:9460-9470.
Manor Y, Nadim F, Abbott LF, Marder E (1997) Temporal dynamics of graded synaptic transmission in the lobster stomatogastric ganglion. J Neurosci 17:5610-5621.
Marder E, Thirumalai V (2002) Cellular, synaptic and network effects of neuromodulation. Neural Netw 15:479-493.
Marder E, Bucher D (2007) Understanding circuit dynamics using the stomatogastric nervous system of lobsters and crabs. Annu Rev Physiol 69:291-316.
Marder E, Hooper SL, Siwicki KK (1986) Modulatory action and distribution of the neuropeptide proctolin in the crustacean stomatogastric nervous system. J Comp Neurol 243:454-467.
Marder E, Bucher D, Schulz DJ, Taylor AL (2005) Invertebrate central pattern generation moves along. Curr Biol 15:R685-699.

Matveev V, Wang XJ (2000) Differential short-term synaptic plasticity and transmission of complex spike trains: to depress or to facilitate? Cereb Cortex 10:1143-1153.
Miller JP, Selverston AI (1982) Mechanisms underlying pattern generation in lobster stomatogastric ganglion as determined by selective inactivation of identified neurons. II. Oscillatory properties of pyloric neurons. J Neurophysiol 48:1378-1391.
Nadim F, Manor Y (2000) The role of short-term synaptic dynamics in motor control. Curr Opin Neurobiol 10:683-690.
Nicholls J, Wallace BG (1978) Quantal analysis of transmitter release at an inhibitory synapse in the central nervous system of the leech. J Physiol 281:171-185.
Norris BJ, Coleman MJ, Nusbaum MP (1996) Pyloric motor pattern modification by a newly identified projection neuron in the crab stomatogastric nervous system. J Neurophysiol 75:97-108.
Nusbaum MP (2002) Regulating peptidergic modulation of rhythmically active neural circuits. Brain Behav Evol 60:378-387.
Nusbaum MP, Marder E (1989a) A modulatory proctolin-containing neuron (MPN). I. Identification and characterization. J Neurosci 9:1591-1599.
Nusbaum MP, Marder E (1989b) A modulatory proctolin-containing neuron (MPN). II. State-dependent modulation of rhythmic motor activity. J Neurosci 9:1600-1607.
Nusbaum MP, Beenhakker MP (2002) A small-systems approach to motor pattern generation. Nature 417:343-350.
Nusbaum MP, Blitz DM, Swensen AM, Wood D, Marder E (2001) The roles of co-transmission in neural network modulation. Trends Neurosci 24:146-154.
Otsu Y, Shahrezaei V, Li B, Raymond LA, Delaney KR, Murphy TH (2004) Competition between phasic and asynchronous release for recovered synaptic vesicles at developing hippocampal autaptic synapses. J Neurosci 24:420-433.
Pan ZH, Hu HJ, Perring P, Andrade R (2001) T-type Ca(2+) channels mediate neurotransmitter release in retinal bipolar cells. Neuron 32:89-98.
Parker D, Gilbey T (2007) Developmental differences in neuromodulation and synaptic properties in the lamprey spinal cord. Neuroscience 145:142-152.
Perez-Reyes E (2003) Molecular physiology of low-voltage-activated t-type calcium channels. Physiol Rev 83:117-161.
Philipp B, Rogalla N, Kreissl S (2006) The neuropeptide proctolin potentiates contractions and reduces cGMP concentration via a PKC-dependent pathway. J Exp Biol 209:531-540.
Rabbah P, Nadim F (2005) Synaptic dynamics do not determine proper phase of activity in a central pattern generator. J Neurosci 25:11269-11278.
Rabbah P, Nadim F (2007) Distinct synaptic dynamics of heterogeneous pacemaker neurons in an oscillatory network. J Neurophysiol 97:2239-2253.
Rabbah P, Golowasch J, Nadim F (2005) Effect of electrical coupling on ionic current and synaptic potential measurements. J Neurophysiol 94:519-530.
Raper JA (1979) Nonimpulse-mediated synaptic transmission during the generation of a cyclic motor program. Science 205:304-306.
Sakurai A, Katz PS (2003) Spike timing-dependent serotonergic neuromodulation of synaptic strength intrinsic to a central pattern generator circuit. J Neurosci 23:10745-10755.

Sakurai A, Katz PS (2009) State-, timing-, and pattern-dependent neuromodulation of synaptic strength by a serotonergic interneuron. J Neurosci 29:268-279.
Sakurai A, Darghouth NR, Butera RJ, Katz PS (2006) Serotonergic enhancement of a 4-AP-sensitive current mediates the synaptic depression phase of spike timing-dependent neuromodulation. J Neurosci 26:2010-2021.
Shu Y, Hasenstaub A, Duque A, Yu Y, McCormick DA (2006) Modulation of intracortical synaptic potentials by presynaptic somatic membrane potential. Nature.
Soto-Treviño C, Rabbah P, Marder E, Nadim F (2005) Computational model of electrically coupled, intrinsically distinct pacemaker neurons. J Neurophysiol 94:590-604.
Stopfer M, Carew TJ (1996) Heterosynaptic facilitation of tail sensory neuron synaptic transmission during habituation in tail-induced tail and siphon withdrawal reflexes of Aplysia. J Neurosci 16:4933-4948.
Stout AK, Li-Smerin Y, Johnson JW, Reynolds IJ (1996) Mechanisms of glutamate-stimulated Mg2+ influx and subsequent Mg2+ efflux in rat forebrain neurones in culture. J Physiol 492 (Pt 3):641-657.
Swensen AM, Marder E (2000) Multiple peptides converge to activate the same voltage-dependent current in a central pattern-generating circuit. J Neurosci 20:6752-6759.
Swensen AM, Marder E (2001) Modulators with convergent cellular actions elicit distinct circuit outputs. J Neurosci 21:4050-4058.
Thirumalai V, Prinz AA, Johnson CD, Marder E (2006) Red pigment concentrating hormone strongly enhances the strength of the feedback to the pyloric rhythm oscillator but has little effect on pyloric rhythm period. J Neurophysiol 95:1762-1770.
Tohidi V, Nadim F (2009) Membrane resonance in bursting pacemaker neurons of an oscillatory network is correlated with network frequency. J Neurosci 29:6427-6435.
Tseng HA, Nadim F (2010) The membrane potential waveform of bursting pacemaker neurons is a predictor of their preferred frequency and the network cycle frequency. J Neurosci 30:10809-10819.
Tsodyks M, Uziel A, Markram H (2000) Synchrony generation in recurrent networks with frequency-dependent synapses. J Neurosci 20:RC50.
Warzecha AK, Kurtz R, Egelhaaf M (2003) Synaptic transfer of dynamic motion information between identified neurons in the visual system of the blowfly. Neuroscience 119:1103-1112.
Weaver AL, Hooper SL (2003) Relating network synaptic connectivity and network activity in the lobster (Panulirus interruptus) pyloric network. J Neurophysiol 90:2378-2386.
Wegener C, Nassel DR (2000) Peptide-induced Ca(2+) movements in a tonic insect muscle: effects of proctolin and periviscerokinin-2. J Neurophysiol 84:3056-3066.
Weimann JM, Meyrand P, Marder E (1991) Neurons that form multiple pattern generators: identification and multiple activity patterns of gastric/pyloric neurons in the crab stomatogastric system. J Neurophysiol 65:111-122.
Zador AM, Dobrunz LE (1997) Dynamic synapses in the cortex. Neuron 19:1-4.

Zhou L, Zhao S, Nadim F (2007) Neuromodulation of short-term synaptic dynamics examined in a mechanistic model based on kinetics of calcium currents. Neurocomputing 70:2050-2054.
Zirpel L, Baldwin D, Graubard K (1993) Nickel induces oscillatory behavior and enhanced synaptic and electrotonic transmission between stomatogastric neurons of Panulirus interruptus. Brain Res 617:205-213.
Zucker RS (1999) Calcium- and activity-dependent synaptic plasticity. Curr Opin Neurobiol 9:305-313.
Zucker RS, Regehr WG (2002) Short-term synaptic plasticity. Annu Rev Physiol 64:355-405.

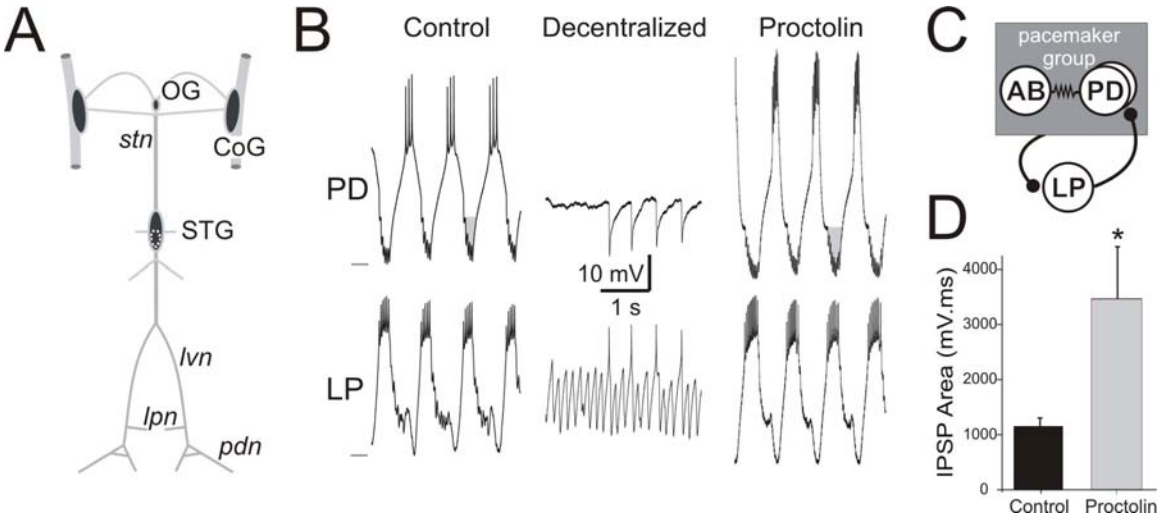

Figure 1 Proctolin enhances the pyloric rhythm. **A.** Schematic diagram of the stomatogastric nervous system. The paired commissural ganglia (COGs) and esophageal ganglion (OG) contain modulatory projection neurons that send axons to the stomatogastric ganglion (STG) through the stomatogastric nerve (*stn*). **B.** Intracellular traces recorded in the normal ongoing pyloric rhythm with intact descending neuromodulatory inputs show the rhythmic alternation of the PD and LP neurons (Control). Blocking or cutting the *stn* removes all descending neuromodulatory input to the STG and disrupts the pyloric rhythm (Decentralized). Bath application of 10^{-6} M proctolin recovers the pyloric rhythm, increases the amplitude of the slow wave oscillations in the PD and LP neurons and increases the spike frequency and number of spikes per burst (Proctolin). Line segments indicate the baselines for the membrane oscillations of PD (−56 mV) and LP (−59 mV) recorded in Control. **C.** A simplified diagram of the pyloric network shows the pacemaker group consisting of the anterior burster (AB) and a pair of PD neurons coupled strongly with electrical synapses (gap junctions) and synaptically inhibiting the follower neuron LP. The LP neuron in turn inhibits the two PD neurons, producing a reciprocally inhibitory sub-network between the pacemaker group and the LP neuron. **D.** A cursory examination of the size of the IPSPs resulting from the LP to PD synapse (gray regions marked in Fig. 1B) shows that during ongoing oscillations proctolin strengthens the synapse compared to control conditions (Student's t-test, $p<0.01$, N=5). Due to variability of IPSP amplitudes during ongoing activity, the IPSP areas were compared.

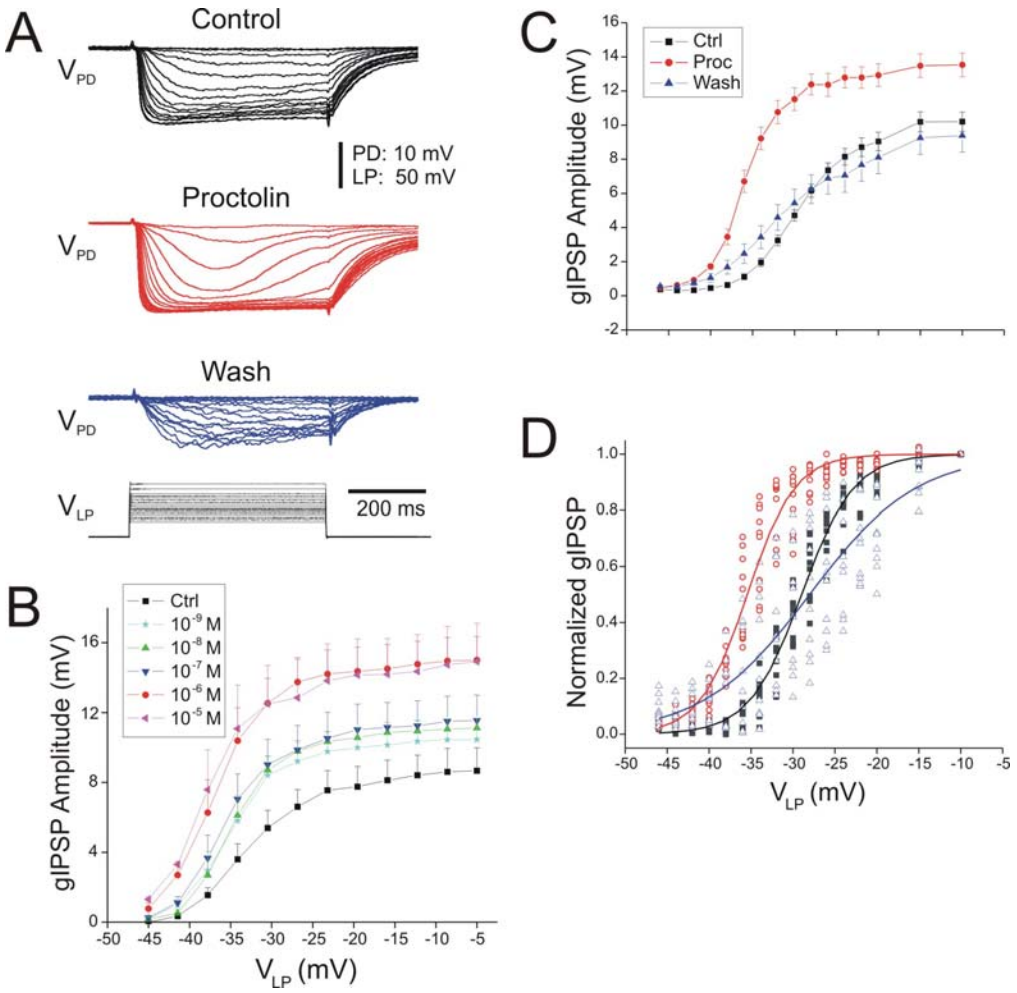

Figure 2 Proctolin strengthens the graded component of the LP to PD synapse. **A.** The LP neuron was voltage-clamped at -60 mV and 500 ms depolarizing square pulses with increasing amplitudes up to 0 mV (V_{LP}) were used to activate the LP to PD synapse in Control, 10^{-6} M Proctolin and Wash. The resulting graded IPSP (gIPSP) recorded in the PD neuron (V_{PD}) increased as the amplitude of the V_{LP} pulse increased for all conditions and was always larger in Proctolin. The enhancement of the synaptic strength was reversible after a 45 minute wash. **B.** The peak amplitudes of gIPSPs were plotted against the V_{LP} pulse values to obtain the synaptic input-output curves in control and in different doses of proctolin. The amplitudes of gIPSPs were augmented in proctolin in a dose dependent manner but saturated at ~10^{-6} M. **C.** The synaptic input-output curve showed a sigmoidal dependency on the presynaptic voltage for both control and proctolin (10^{-6} M). Proctolin significantly strengthened gIPSPs of the LP to PD synapse for presynaptic amplitudes ≥ 35 mV compared to control and wash (two-way ANOVA post-hoc Tukey analysis, $p < 0.01$ for $V_{LP} = -35$ to -10 mV; N=6). **D.** The amplitude of the individual gIPSPs in each preparation was normalized to the gIPSP. Each data point (black: control; red: proctolin; blue: wash) indicates a single measurement from six preparations and these measurements were fit with Boltzmann type equations. Proctolin shifted the midpoint of the input-output curve by ~5.5 mV to more negative membrane potentials (V_{half} in mV—Ctrl: -29.0±0.11; Proc: -35.4±0.14; Wash: -28.0 ±0.44) but did not significantly change the slope of this curve, although the slope became shallower after wash (k_{half} in mV—Ctrl: -3.11±0.10; Proc: -2.83±0.12; Wash: -6.36 ±0.45).

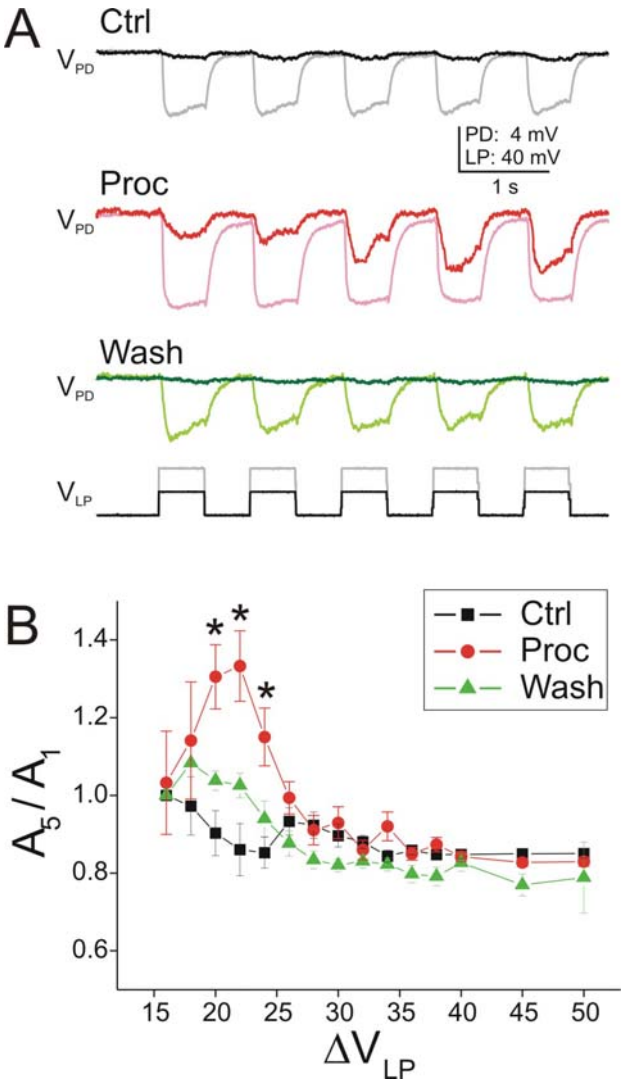

Figure 3 Proctolin modulates the short-term dynamics of the LP to PD graded synapse in response to different amplitude depolarizations. **A.** LP neuron was voltage-clamped at -60 mV and stimulated with a series of five square pulses of 20 mV (V_{LP}: black trace) or 40 mV (V_{LP}: gray trace) amplitudes in control, proctolin and wash. In control and wash, the LP to PD synapse was depressing. In proctolin, in response to 20 mV presynaptic depolarization, the gIPSPs in the PD neuron showed facilitation **B.** The ratio of the 5th to the 1st mean gIPSP amplitude (A_5/A_1) calculated for all presynaptic depolarizations with an inter-pulse interval of 500 ms plotted against presynaptic pulse amplitudes (ΔV_{LP}). In control (black), the ratio A_5/A_1 was slightly less than one for all values of presynaptic pulse amplitudes (ΔV_{LP}), indicating that the synapse was always depressing. In contrast, in the presence of proctolin (red), the A_5/A_1 ratios in response to pulse amplitudes between 20 and 24 mV were greater than 1 while the ratios in response to larger pulse amplitudes were less than 1, indicating facilitation and depression, respectively (2-way ANOVA with post hoc Tukey test showing $p<0.001$ between ctrl and proctolin and $p<0.008$ between control and wash for $\Delta V_{LP} = 20$, 22 and 24 mV; not significant at other ΔV_{LP}).

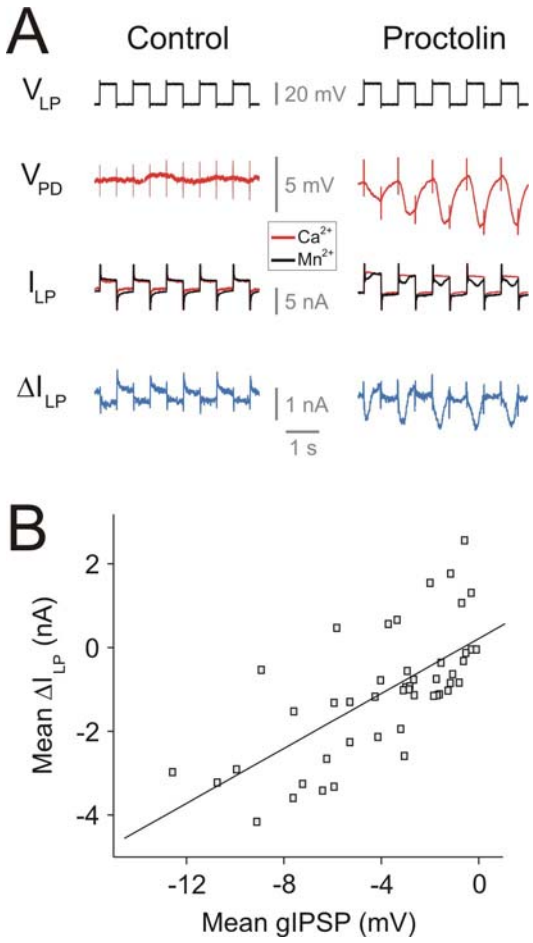

Figure 4 Proctolin caused a facilitation of the LP to PD graded inhibitory postsynaptic potentials in response to low-amplitude presynaptic depolarizing pulses, which is associated with the activation of a Ca^{2+}-like inward current. **A.** The presynaptic currents in the LP neuron (I_{LP}) are measured in Ca^{2+} saline (black) and in Mn^{2+} saline (red) using a train of low-amplitude presynaptic voltage pulses. The difference between the two measured currents (ΔI_{LP}= $I_{LP:Ca2+}$ - $I_{LP:Mn2+}$) reveals a new inward current activated in proctolin. A series of low amplitude presynaptic depolarizing pulses cause little response in postsynaptic neuron PD in control. Proctolin strengthened and caused facilitation in the PD neuron in response to low amplitude presynaptic depolarizing pulses. ΔI_{LP} also increased with each pulse. V_{PD} is not shown in Mn^{2+} because synaptic transmission was blocked. **B.** The mean value (area divided by pulse duration) of the presynaptic inward current ΔI_{LP} in response to each pulse plotted against the mean value of the postsynaptic potentials V_{PD} (IPSP area divided by pulse duration). Linear regression fit shows the correlation between the presynaptic inward current and the postsynaptic potentials (R=0.69, P<0.001, N=9).

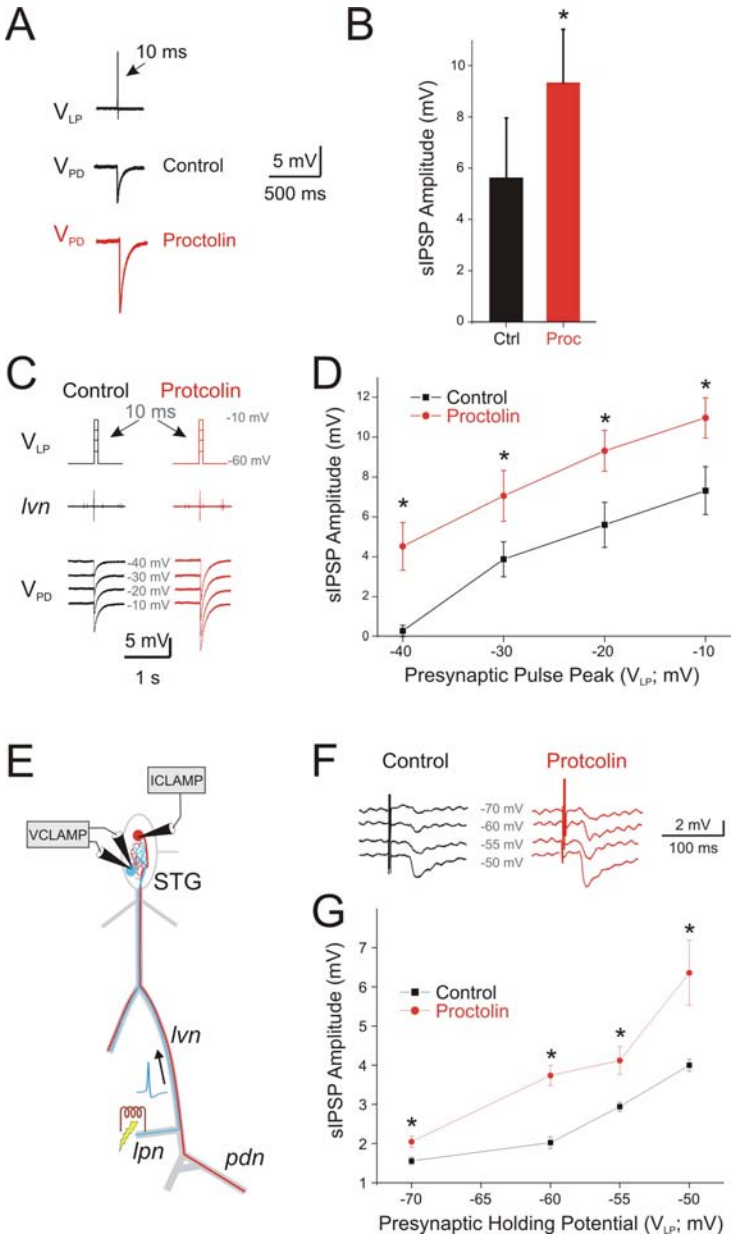

Figure 5 The strength of unitary spike-mediated IPSPs (sIPSPs) is enhanced by proctolin. **A.** The LP neuron was voltage-clamped at -60 mV and stimulated with one short square pulse of duration 10 ms and amplitude 30 mV. The resulting sIPSP was recorded in PD neuron (V_{PD}) in control and in proctolin (10^{-6} M). **B.** Bath application of proctolin significantly enhanced the amplitude of the unitary sIPSPs (Student's t-test, $p<0.001$; N=6). **C.** The LP neuron was voltage-clamped at -60 mV and stimulated with one short square pulse of duration 10 ms and increasing amplitude (to peak voltages V_{LP} = -40, -30, -20, -10 mV). A single action potential spike elicited by the 10 ms voltage pulse was recorded on the nerve *lvn*. The resulting sIPSPs were recorded in PD neuron (V_{PD}) in control and in proctolin (10^{-6} M). **D.** The amplitude of sIPSPs in response to the 10 ms voltage pulse in control and proctolin increased if the amplitude of this short presynaptic voltage pulse was increased. Bath application of proctolin significantly increased the sIPSP amplitude for all values of the presynaptic pulse amplitudes (two-way ANOVA post-hoc Tukey analysis, $p<0.05$, N=8). **E.** Schematic diagram showing how antidromic spikes were elicited in the LP neuron. The LP neuron (blue) soma was voltage-clamped and the PD neuron (red) was recorded in current clamp. To elicit antidromic spikes, the lateral pyloric nerve (*lpn*) which contains the axon of the LP neuron but not that of the PD neuron was stimulated. **F.** The LP neuron was voltage-clamped at different holding potentials (V_{LP}=-70, -60, -55 and -50 mV). The sIPSPs were recorded in PD neuron in response to antidromic spikes in the LP neuron in control and proctolin (10^{-6} M). **G.** The peak sIPSP amplitude plotted against the holding potentials of the LP neuron in control and in proctolin. As the holding potential of the LP neuron was increased, the amplitude of sIPSPs in the PD neuron also increased in both control and 10^{-6} M proctolin. In the presence of proctolin, the sIPSPs were larger in comparison to control (two-way RM-ANOVA, $p<0.05$, N=5).

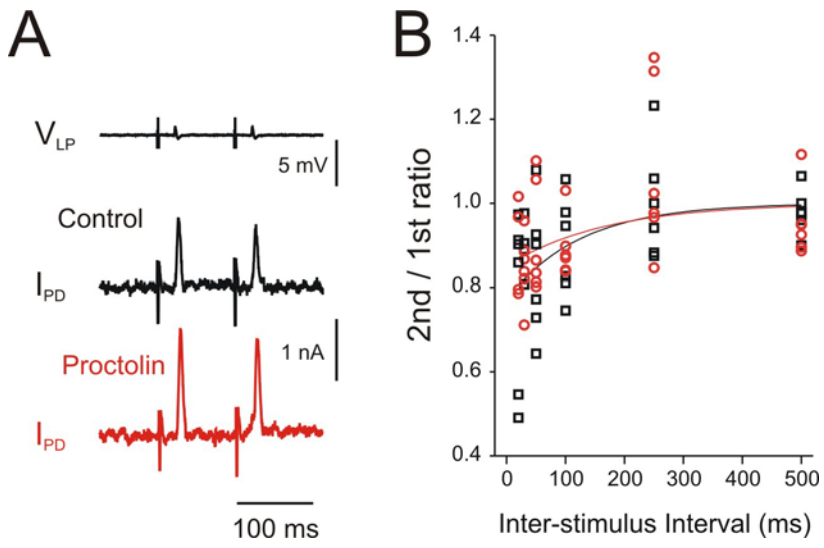

Figure 6 Proctolin does not have a significant effect on the short-term dynamics of the sIPSPs. **A.** The LP and PD neurons were voltage clamped at a holding potential of -50 mV. The resulting spike-mediated synaptic currents in the PD neuron in response to two successive antidromic spikes with a 100 ms interval were recorded and repeated 10 times. The averaged traces were shown in control (black) and proctolin (red). The spike-mediated synaptic current (sIPSC) amplitude was significantly strengthened by proctolin (Ctrl: 0.49±0.02 nA, Proc: 1.3±0.1 nA; Student's t-test, $P<0.01$, N=4) **B.** The ratio of the sIPSC amplitudes in response to the first two successive antidromic spikes plotted against inter-spike interval in control and in proctolin. The exponential fit curves ($y = 1 - Ae^{-x/B}$) were plotted in control (black: A=-0.23, B=125) and in proctolin (red: A=-0.15, B=167). Proctolin did not cause a significant change in the short-term dynamics compared to control.

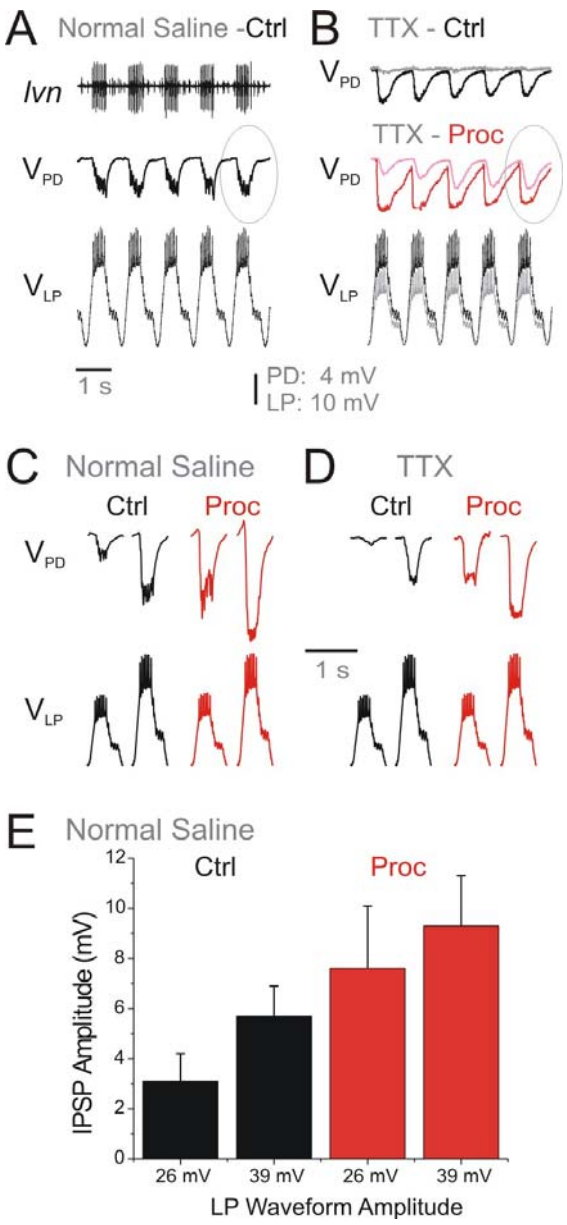

Figure 7 Proctolin strengthens the total LP to PD synaptic IPSP measured using prerecorded realistic waveforms in the LP neuron. **A.** After decentralizing the preparation, the LP neuron was voltage-clamped at a holding potential of -60 mV and injected with a voltage profile constructed using a pre-recorded realistic LP neuron waveform (V_{LP}) with a total amplitude 39 mV (1.5 times the recorded amplitude). The resulting IPSP was measured in the PD neuron (V_{PD}). The simulated action potentials of the realistic waveform resulted in real action potentials in the presynaptic LP neuron which were recorded on the nerve *lvn*. Voltage scalebar applies to panels *A-D*. **B.** Application of the realistic waveform in TTX with total amplitude of 26 mV (same as recorded amplitude; gray V_{LP} trace) resulted in synaptic facilitation of the gIPSP in proctolin (gray V_{PD} trace) but not control saline (gray V_{PD} trace). In contrast, application of the waveform at 39 mV (black) resulted in slight depression of the gIPSP both in control (black) and in proctolin (red). **C.** In normal saline, the LP waveform was applied periodically with total amplitude of 26 mV or 39 mV. The resulting IPSP, a combination of the graded and spike-mediated components, was measured in the PD neuron in control saline (black) or in the presence of proctolin (red). The responses shown are after at least four cycles of the presynaptic waveform (circled in *A* and *B*) when the IPSP has reached its stationary state. **D.** In TTX, the same LP waveform was applied periodically with total amplitude of 26 mV or 39 mV. The resulting IPSP in this case consists only of the graded component. All responses shown in *C* and *D* were measured in the same preparation. E. Mean values of the peak IPSP as shown in panel *C* indicate a significant increase with both amplitude and proctolin (two-way RM-ANOVA; $p<0.05$).

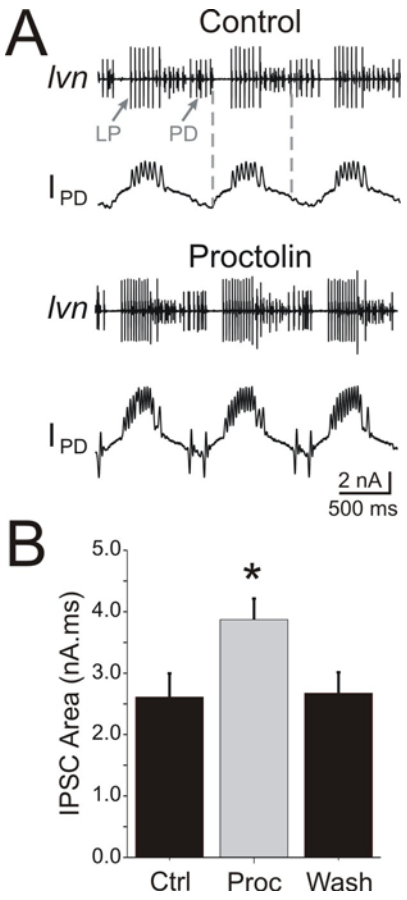

Figure 8 Proctolin enhances the LP to PD synapse during the ongoing pyloric rhythm. **A.** The traces of extracellular recordings from *lvn* show the ongoing rhythm activity of the pyloric network in control and in proctolin (10^{-6} M). One of the two PD neurons was voltage clamped at a holding potential of -55 mV; the resulting synaptic currents were recorded in this PD neuron in control and in proctolin. **B.** The synaptic response in PD neuron was integrated from the end of a PD burst to the start of the following PD burst (vertical dashed lines in A). When necessary, DC current was injected in the second PD neuron to bring the cycle period to 1 sec in all measurements. The IPSC area was significantly larger in proctolin than control or wash (one-way ANOVA, $p<0.01$, N=5).